

# AICON: A program for calculating thermal conductivity quickly and accurately<sup>☆,☆☆</sup>

Tao Fan<sup>\*</sup>, Artem R. Oganov

Skolkovo Institute of Science and Technology, 3 Nobel St., 121205 Moscow, Russia

## ARTICLE INFO

### Article history:

Received 20 August 2019  
 Received in revised form 11 November 2019  
 Accepted 20 November 2019  
 Available online 27 November 2019

### Keywords:

Lattice thermal conductivity  
 Debye–Callaway model  
 Phonon relaxation time

## ABSTRACT

AICON (*Ab Initio* Conductivities) is a program written in Python for computing lattice thermal conductivity of crystalline bulk materials using the modified Debye–Callaway model. Building upon the traditional Debye–Callaway theory, the modified model obtains the lattice thermal conductivity by averaging the contributions from acoustic and optical branches based on their specific heat. The only inputs of this program are the phonon spectrum, phonon velocity and Grüneisen parameter, all of which can be calculated using third-party *ab initio* packages, making the method fully parameter-free. This leads to a fast and accurate evaluation and enables high-throughput calculations of lattice thermal conductivity even in large and complex systems. In addition, this program calculates the specific heat and phonon relaxation times for different scattering processes, which will be beneficial for understanding the phonon transfer behavior.

### Program summary

**Program Title:** AICON

**Program Files doi:** <http://dx.doi.org/10.17632/s9b8y8t92c.1>

**Licensing provisions:** GNU General public license 3

**Programming language:** Python3

**External routines/libraries:** Numpy, Scipy, spglib, pymatgen

**Nature of problem:** The calculation of lattice thermal conductivity from first principles with an anharmonic approximation requires a large number of calculations to construct the third-order force constants matrix, which could be prohibitively long time.

**Solution method:** Modified Debye–Callaway model, where only the phonon spectrum, phonon velocity and Grüneisen parameter are needed. The acoustic branch and optic branch are both considered to obtain the final lattice thermal conductivity.

© 2019 Elsevier B.V. All rights reserved.

## 1. Introduction

Studies of thermal conductivity and its behavior under extreme conditions play an important role in various technological and scientific applications, including thermoelectricity, heat management, and investigations of the deep Earth (mantle and core of the Earth). Calculations of thermal conductivity that use as input only the basic information (such as crystal structure) and do not require any other parameters obtained from experiments, while maintaining a sufficient accuracy, could be especially helpful in such research. Over the years, several approaches were proposed

to fulfil this objective, e.g. the relaxation time approximation (RTA), iterative solution of the Boltzmann transport equation (BTE) and *ab initio* molecular dynamics. These methods are used in such software tools as Phono3py [1], ShengBTE [2], LAMMPS. However, all these approaches need large computing resources. Addressing these issues, here we present a small but robust computer program that calculates the lattice thermal conductivity, which is the phonon contribution of the thermal conductivity of bulk crystalline materials. The program works fast and shows good accuracy.

Lattice thermal conductivity can be calculated directly using the temperature gradient from the nonequilibrium molecular dynamics (MD) simulation at a given heat current [3,4] or from the equilibrium MD simulations using the Green–Kubo method [5]. However, MD simulations need a large supercell to take into account crucially important long-wavelength phonons, and long simulation time is needed to converge the autocorrelation function. The second method to calculate lattice thermal conductivity

<sup>☆</sup> This paper and its associated computer program are available via the Computer Physics Communication homepage on ScienceDirect (<http://www.sciencedirect.com/science/journal/00104655>).

<sup>☆☆</sup> The review of this paper was arranged by Prof. D.P. Landau.

<sup>\*</sup> Corresponding author.

E-mail address: [Tao.Fan@skoltech.ru](mailto:Tao.Fan@skoltech.ru) (T. Fan).

is solving the phonon Boltzmann transport equation (PBTE), for which the most convenient way is to use the relaxation time approximation (RTA) along with the Debye approximation. Based on the RTA, a full iterative solution to the PBTE was developed [6]. However, these calculations need the second- and third-order interatomic force constants. Although density functional theory (DFT) is a convenient tool for accurately calculating the interatomic interactions in many cases, obtaining the third-order force constants used in the description of anharmonicity in phonon-phonon processes is still time-consuming. Another way to calculate lattice thermal conductivity  $\kappa_L$  from first principles is the Debye–Callaway model.

In 1959, Callaway proposed a solution for the PBTE based on three assumptions [7]: first, only four scattering mechanisms are considered, including point impurities (isotopic disorder), normal three-phonon processes, Umklapp processes and boundary scattering; second, all phonon scattering processes can be represented by frequency-dependent relaxation times; third, the crystal vibrational spectrum is isotropic and dispersionless (assuming linear dependence of the acoustic frequencies on the wavevector). Based on this model,  $\kappa_L$  of germanium was calculated in the temperature range of 2 K to 100 K. The results showed reasonable agreement with the experiments for both normal and isotopically pure material. Asen-Palmer [8] modified the Debye–Callaway model by accounting for the contributions of longitudinal and transverse acoustic branches differently. In addition, this approach uses six freely adjustable parameters for longitudinal and transverse modes in order to include the anharmonic effect and contributions from the boundary and isotope scattering. Unfortunately, these models lack the predictive power since they incorporate parameters that are either fitted to experimental data or freely adjustable. Morelli et al. [9] modeled lattice thermal conductivity and isotope effect in Ge, Si, and diamond using an approach similar to that of Asen-Palmer. However, they used the known phonon dispersion relations of these crystals to derive all the necessary parameters except the Grüneisen parameter. Recently, Zhang [10] developed a first-principles Debye–Callaway approach, where all the parameters (i.e., the Debye temperature  $\Theta$ , phonon velocity  $v$  and Grüneisen parameter  $\gamma$ ) can be directly calculated from the vibrational properties of compounds within the quasi-harmonic approximation.

In this paper we present a software package, *AICON*, for calculating lattice thermal conductivity from the phonon dispersion curves obtained *ab initio*. However, unlike the traditional Debye–Callaway model which only considers acoustic branches, our modified method also accounts for the contribution from optical branches, which could be as large as 20% to 50% at high temperatures, according to Slack [11]. We obtain the lattice thermal conductivity by averaging the contributions from the acoustic branches and optical branches based on their specific heat  $c_v$ . In addition, our software package can calculate the phonon–phonon relaxation times for different scattering mechanisms (including  $N$  process,  $U$  process and isotope scattering), which is important for the deeper analysis of the heat transfer.

The paper is structured as follows. In Section 2 we introduce the mathematical formalism and methodological choices behind *AICON*. Section 3 includes tests for three different systems. We present our main conclusions and discuss future directions for development in Section 4.

## 2. Methodology

### 2.1. *AICON* workflow

The software presented in this paper enables approximate and highly efficient lattice thermal conductivity calculation from first

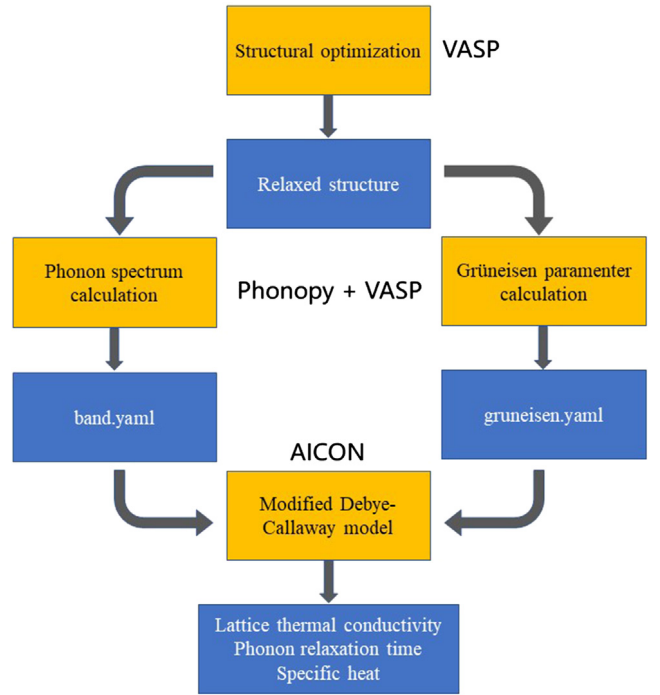


**Fig. 1.** The workflow of lattice thermal conductivity calculation using *AICON*. Gold boxes represent steps of the calculation, blue boxes for the results of these steps, and computer programs are denoted as black text outside of the box. (For interpretation of the references to color in this figure legend, the reader is referred to the web version of this article.)

principles. The main improvement of our method compared with the older Callaway model is that the contribution from the optical branches is included and all the necessary physical quantities including Debye temperature, phonon velocity and Grüneisen parameter are obtained by first-principles calculations. The only inputs needed by *AICON* are phonon dispersion curves, phonon velocity and mode Grüneisen parameters. Our program relies completely on external tools (such as Phonopy [12]) to generate them.

We recommend to use VASP [13] combined with Phonopy to do the DFT calculations. A summary of our workflow, starting with structure relaxation of each material and ending with the calculation of  $\kappa_L$ , is shown in Fig. 1.

### 2.2. Modified Debye–Callaway model

Following the approach used by Morelli [9], we update the formalism used to calculate lattice thermal conductivity. The total lattice thermal conductivity  $\kappa$  is the weighted average of the acoustic branches (one longitudinal  $\kappa_{LA}$ , two transverse  $\kappa_{TA}$  and  $\kappa_{TA'}$ ) and one pseudo-optic branch ( $\kappa_O$ ):

$$\kappa = \frac{c_V^{aco}}{c_V^{aco} + c_V^{opt}} \times \frac{\kappa_{LA} + \kappa_{TA} + \kappa_{TA'}}{3} + \frac{c_V^{aco}}{c_V^{aco} + c_V^{opt}} \times \kappa_O \quad (1)$$

where  $\kappa_i = \kappa_{i1} + \kappa_{i2}$ , with  $i$  denoting  $LA$ ,  $TA$ ,  $TA'$  and optic modes  $O$ .  $c_V^{aco}$  and  $c_V^{opt}$  are specific heat of acoustic and optical branches, which will be explained later. The partial conductivities  $\kappa_{i1}$  and  $\kappa_{i2}$  are the common Debye–Callaway terms:

$$\kappa_{i1} = C_i T^3 \int_0^{\Theta_i/T} \frac{\tau_c^i(x) x^4 e^x}{(e^x - 1)^2} dx \quad (2a)$$

$$\kappa_{i2} = C_i T^3 \frac{\int_0^{\Theta_i/T} \frac{\tau_c^i(x) x^4 e^x}{(e^x - 1)^2} dx}{\int_0^{\Theta_i/T} \frac{\tau_N^i(x) \tau_R^i(x) (e^x - 1)^2}{\tau_N^i(x) \tau_R^i(x) (e^x - 1)^2} dx} \quad (2b)$$

In these expressions,  $\theta_i$  is the Debye temperature for each phonon branch,  $C_i = k_B^4 / (2\pi^2 \hbar^3 v_i)$  and  $x = \hbar\omega / k_B T$ , where  $\hbar$  is the Planck constant,  $k_B$  is the Boltzmann constant,  $\omega$  is the phonon frequency, and  $v_i$  is the phonon velocity for each branch;  $(\tau_N^i)^{-1}$  is the scattering rate of the normal phonon process,  $(\tau_R^i)^{-1}$  is the total scattering rate of all the resistive scattering processes, and  $(\tau_C^i)^{-1} = (\tau_N^i)^{-1} + (\tau_R^i)^{-1}$ . According to Callaway,  $(\tau_R^i)^{-1}$  should equal the sum of the scattering rates of the phonon-phonon Umklapp scattering, isotope point defect scattering, and scattering from the crystal boundary. In our model, only the Umklapp scattering and isotope scattering are considered, so that  $(\tau_R^i)^{-1} = (\tau_U^i)^{-1} + (\tau_I^i)^{-1}$ . For most practical applications like thermoelectricity, where the temperature is usually above 300 K, it is reasonable to omit boundary scattering because it becomes significant only at very low temperatures, usually tens of Kelvins.

2.2.1. Phonon-phonon normal scattering

Although the normal phonon scattering is not a resistive process, it can redistribute the momentum and energy among phonons and influence other resistive scattering processes (such as the Umklapp scattering). Following the approach of Asen-Palmer [8], the appropriate forms for longitudinal and transverse acoustic phonons are

$$[\tau_N^L(x)]^{-1} = B_N^L \left(\frac{k_B}{\hbar}\right)^2 x^2 T^5 \tag{3a}$$

and

$$[\tau_N^T(x)]^{-1} = B_N^T \left(\frac{k_B}{\hbar}\right)^2 x T^5 \tag{3b}$$

with the magnitudes  $B_N$  depending on the phonon velocity  $v$  and Grüneisen parameter  $\gamma$ ,

$$B_N^L = \frac{k_B^3 \gamma_L^2 V}{M \hbar^2 v_L^5} \tag{4a}$$

and

$$B_N^T = \frac{k_B^4 \gamma_T^2 V}{M \hbar^3 v_T^5} \tag{4b}$$

where  $M$  is the mean atomic mass in the crystal and  $V$  is the volume per atom. A more general case and further discussion are included in the Appendix of Ref. [9]. For the optical branch, we assume the same formula as for the longitudinal acoustic branch.

2.2.2. Phonon-phonon Umklapp scattering

The phonon-phonon Umklapp processes dominate at high temperatures, following an exponential behavior. According to Morelli [9], the Umklapp scattering rate for longitudinal and transverse acoustic phonons is:

$$[\tau_U^i(x)]^{-1} = B_U^i \left(\frac{k_B}{\hbar}\right)^2 x^2 T^3 e^{-\theta_i/3T} \tag{5a}$$

where

$$B_U^i = \frac{\hbar \gamma_i^2}{M v_i^2 \theta_i} \tag{5b}$$

The Umklapp scattering rate thus depends on Debye temperature, phonon velocity, and Grüneisen parameter of each branch. Again, we assume the optical branch to be described by the same formula as the longitudinal acoustic branch.

2.2.3. Phonon-isotope scattering

According to Klemens [14], the scattering rate of mass fluctuation due to the presence of isotopes should take the form

$$[\tau_I^i(x)]^{-1} = \frac{V k_B^4 \Gamma}{4\pi \hbar^4 v_i^3} x^4 T^4 \tag{6}$$

Therefore, the isotope scattering rate also depends on the phonon velocity. The mass fluctuation phonon scattering parameter  $\Gamma$  for a single element composed of several naturally occurring isotopes is

$$\Gamma = \sum_i c_i \left[ \frac{m_i - \bar{m}}{\bar{m}} \right]^2 \tag{7a}$$

where

$$\bar{m} = \sum_i c_i m_i \tag{7b}$$

$m_i$  is the atomic mass of the  $i$ th isotope and  $c_i$  is the fractional atomic natural abundance. For a compound including  $N$  different elements,

$$\Gamma(AB\dots) = N \left[ \left( \frac{M_A}{M_A + M_B + \dots} \right)^2 \Gamma(A) + \left( \frac{M_B}{M_A + M_B + \dots} \right)^2 \Gamma(B) + \dots \right] \tag{8}$$

where  $M_i$  ( $i = A, B, \dots$ ) denotes the average atomic mass of element  $i$ .

2.2.4. Specific heat

The specific heat is usually calculated using Debye model, which is only suitable for the acoustic branches. For structures whose primitive cell contains more than one atom ( $p > 1$ ), a more accurate method would be using the Debye model for the acoustic branches, while approximating the optical branches by the Einstein model. Then, the specific heat is

$$c_V^{aco} = 3 \frac{N}{V} k_B f_D \left( \frac{\Theta_D}{T} \right) \tag{9a}$$

$$c_V^{opt} = (3p - 3) \frac{N}{V} k_B f_E \left( \frac{\Theta_E}{T} \right) \tag{9b}$$

$$f_D(x) = \frac{3}{x^3} \int_0^x \frac{y^4 e^y dy}{(e^y - 1)^2} \tag{9c}$$

and

$$f_E(x) = x^2 \frac{e^x}{(e^x - 1)^2} \tag{9d}$$

where  $\Theta_D$  is the Debye temperature,  $\Theta_E$  is the Einstein temperature,  $N$  is the number of primitive cells,  $f_D$  and  $f_E$  are the Debye function and Einstein function respectively.

2.2.5. Debye temperature, Grüneisen parameter, and phonon velocity

The lattice thermal conductivity is a function of the Debye temperature  $\theta_i$ , Grüneisen parameter  $\gamma_i$  and phonon velocity  $v_i$  of each phonon branch (Eqs. (1)–(9)), the parameters that can be readily obtained from an external software such as Phonopy.

For Debye temperature, we select the highest frequency of each branch to calculate  $\theta_i$ :

$$\theta_i = \frac{\hbar \omega_i^{max}}{k_B} \tag{10}$$

The Debye temperature  $\Theta_D$  in Eq. (9a) could, in principle, calculated from the specific heat at low temperatures or, equivalently, from the elastic constants. However, this determination is implicitly based on the assumption that acoustic frequencies depend linearly on the wavevector, and will overestimate the maximum acoustic frequency. Here we determine the Debye temperatures from the maximum  $\theta_i$  of the three acoustic branches, and this gives  $\Theta_D$  somewhat lower than standard values of the Debye temperature.

**Table 1**  
The characteristic temperatures ( $\theta$ ), phonon velocities ( $v$ ) and Grüneisen parameters ( $\gamma$ ) of the transverse, longitudinal acoustic branches and optical branch of Si, diamond and SnSe.

Material	$\theta_{TA}$ (K)	$\theta_{TA'}$ (K)	$\theta_{LA}$ (K)	$\theta_O$ (K)	$v_{TA}$ (m s <sup>-1</sup> )	$v_{TA'}$ (m s <sup>-1</sup> )	$v_{LA}$ (m s <sup>-1</sup> )	$v_O$ (m s <sup>-1</sup> )	$\gamma_{TA}$	$\gamma_{TA'}$	$\gamma_{LA}$	$\gamma_O$
Si	289.4	315.3	576.9	723.2	4635.7	4931.3	8424.0	385.2	0.57	0.37	1.04	1.18
C	1308.5	1415.5	1561.8	1872.7	11803.0	12236.6	17694.1	423.8	0.54	0.82	1.05	1.07
SnSe	70.2	70.2	71.4	197.3	2212.5	2194.7	2948.9	303.7	16.71	3.32	2.96	0.74

The phonon velocity and Grüneisen parameter of each branch are calculated using a two-step averaging. The results of the Phonopy calculation of the phonon velocity and Grüneisen parameter are a function of band index  $i$  and wavevector  $\mathbf{q}$ , namely  $v(i, \mathbf{q})$  and  $\gamma(i, \mathbf{q})$ . The first average is taken within each high symmetry path of the same branch:

$$v(i, j) = \overline{v(i, \mathbf{q})} \quad (11a)$$

$$\gamma^2(i, j) = \overline{[\gamma(i, \mathbf{q})]^2} \quad (11b)$$

where  $j$  denotes a different high symmetry path in each branch. The second average is taken of these high symmetry paths:

$$v_i = \frac{\sum_j m_j v(i, j)}{\sum_j m_j} \quad (12a)$$

$$\gamma_i = \sqrt{\frac{\sum_j m_j \gamma^2(i, j)}{\sum_j m_j}} \quad (12b)$$

where  $m_j$  is the multiplicity of each high symmetry path, a value related to the symmetry of the structure.

We did not use all the optical branches in the thermal conductivity calculations. Instead, to correspond with the Einstein model and treat the optical branches' contribution as a correction to the original Callaway model, we use a "pseudo-optical" branch, which is an average of the optical branches.  $\Theta_E$  in Eq. (9b) is the characteristic Einstein temperature of this "pseudo-optical" branch.

### 2.3. Settings for first-principles calculations

All the first-principles calculations were performed using the VASP code with the projector-augmented wave (PAW) method [15, 16]. The exchange–correlation energy was approximated by the PBE–GGA functional [17]. For total energy calculations and structure relaxation, the plane wave kinetic energy cutoff was set to 600 eV and the Brillouin zone was sampled using  $\Gamma$ -centered meshes [18] with reciprocal-space resolution of  $2\pi \times 0.03 \text{ \AA}^{-1}$ . Kohn–Sham equations were solved self-consistently with total energy tolerance of  $10^{-7}$  eV/cell and structures were relaxed until the maximum force became less than  $10^{-3}$  eV/Å. For the phonon calculations, a  $2 \times 2 \times 2$  supercell was built and DFPT [19] was used to obtain the second-order interatomic force constants (IFCs). To get Grüneisen parameters, three phonon calculations have to be run: one at the equilibrium volume, the other two at slightly smaller (−0.4%) and larger volume (+0.4%) volumes. For SnSe, the van der Waals correction (IVDW = 11) was included because this material has layered structure.

## 3. Examples

We illustrate the capabilities of AICON by performing calculations for three prototypical systems: (1) carbon in the diamond phase, an insulator with very high thermal conductivity; (2) silicon, the most studied semiconductor with normal thermal conductivity value; (3) tin selenide (SnSe), a famous thermoelectric material with the highest figure of merit achieved in its single crystal, mainly because of its very low thermal conductivity.

### 3.1. Carbon (diamond)

The phonon spectrum of diamond is shown in Fig. 2a. The lattice thermal conductivity of diamond calculated in this work is shown in Fig. 2b in comparison with the measurements reported in two studies [20,21] and the calculation using the full *ab initio* method [22]. We also compare with results of ShengBTE program. The needed second-order force constants file, third-order force constants file and other parameters were obtained from the database [23]. The calculated Debye temperature, phonon velocity and Grüneisen parameter of diamond used with our method are listed in Table 1. We compared these parameters with previous work [9] to make sure these input parameters are correct.

High lattice thermal conductivity of diamond is mainly caused by its very high phonon velocity. In general, our method tends to overestimate the value of the lattice thermal conductivity at low temperatures. For example,  $\kappa_L$  obtained in our calculations at 300 K is  $3180 \text{ W m}^{-1} \text{ K}^{-1}$ , while the experimental value is close to  $2000 \text{ W m}^{-1} \text{ K}^{-1}$ . This is partly because we did not account for boundary scattering, while the Debye temperature of diamond is very high ( $\sim 2000$  K), meaning that 300 K can even be considered as a low temperature. Different isotopic compositions in experiment and calculation could also account for such a difference of the thermal conductivity at low temperatures. At higher temperatures ( $>500$  K), the difference between our calculation results and the reference values is within 10%. Comparing with the results of ShengBTE, we see good agreement at temperatures below 400 K, but at higher temperatures our results are much closer to experiment.

The ratios of the acoustic specific heat to total specific heat ( $R_A$ ) and of the optical specific heat to total specific heat ( $R_O$ ), which can reflect the relative contribution of the acoustic branches and optical branches, are shown in Fig. 2c. Within the temperature range of 200 K–1000 K,  $R_A$  is larger than  $R_O$ , indicating the domination of the acoustic branches. However,  $R_A$  diminishes while  $R_O$  grows as temperature increases, making the contributions from the acoustic and optical branches almost equal above 1000 K.

Fig. 2d shows the phonon relaxation times in the resistive scattering processes, i.e. Umklapp scattering and isotope scattering, for each branch. From these data, we can compare the contribution of different scattering processes and understand the origin of thermal resistivity. For example, in the isotope scattering process, the relaxation times are 5.70E–11 s, 4.64E–11 s and 9.47E–11 s for the TA, TA' and LA branches, respectively. In the Umklapp process, the relaxation times above 300 K are shorter than those in the isotope scattering process for all the acoustic branches, suggesting that Umklapp scattering is stronger than isotope scattering. The relaxation times for optical branches are shorter than those for the acoustic branches by three orders of magnitude, suggesting a very strong scattering of phonons.

### 3.2. Silicon

The calculated phonon spectrum and lattice thermal conductivity of Si are shown in Fig. 3a and b, respectively, the latter providing a comparison with the experimental results for the

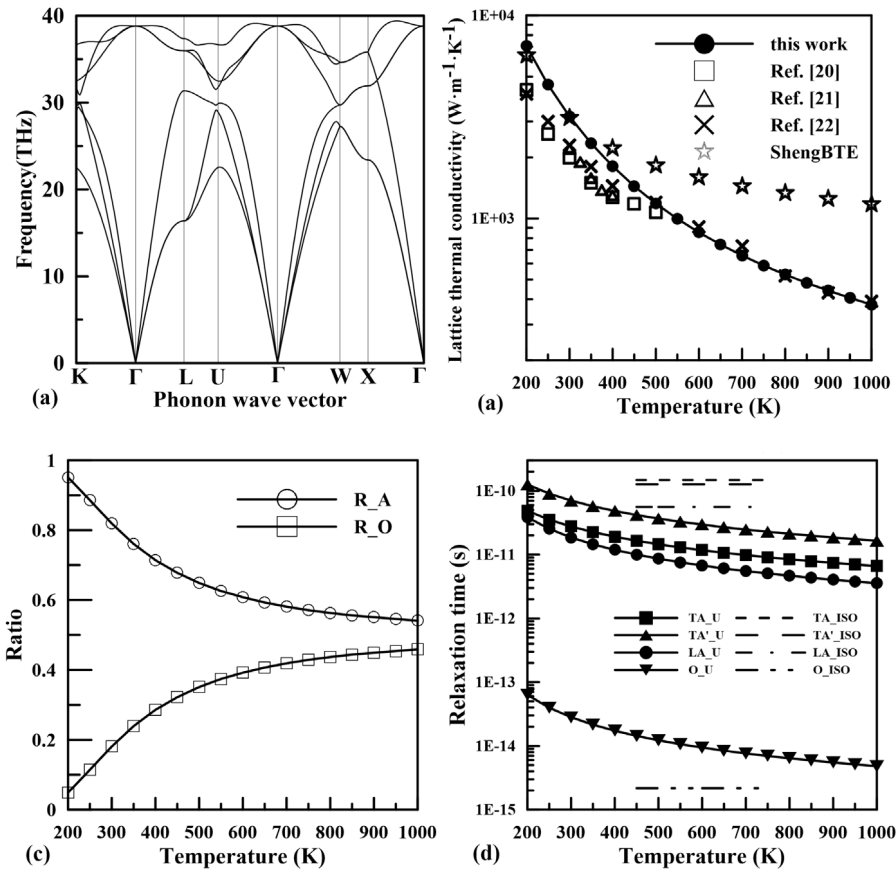


**Fig. 2.** (a) Phonon spectrum of diamond. (b) Lattice thermal conductivity of diamond calculated by our method compared with the experimental and full *ab initio* results. (c) Percentage of specific heat from the acoustic and optical branches in the total specific heat of diamond. (d) Phonon relaxation times for the resistive scattering processes.

natural Si isotopic composition [24,25] and results calculated from ShengBTE. The results are in close agreement with the experimentally measured values at temperatures above 200 K. For example, at 300 K, the lattice thermal conductivity calculated using our method is  $130 \text{ W m}^{-1} \text{ K}^{-1}$ , while the experimental value is  $140 \text{ W m}^{-1} \text{ K}^{-1}$ – $143 \text{ W m}^{-1} \text{ K}^{-1}$ , which shows the difference of 7%–9%. For temperatures below 200 K, the difference may be larger due to the neglect of boundary scattering in the calculations and possible difference of the isotopic composition. Compared with ShengBTE, both methods give close results in the calculated temperature range.

The ratios of the acoustic specific heat to total specific heat,  $R_A$ , and that of the optical specific heat to total specific heat,  $R_O$ , are shown in Fig. 3c. The two ratios converge as temperature increases. Similar to diamond, in the temperature range 200 K–1000 K,  $R_A$  is larger than  $R_O$ , indicating the dominance of the acoustic branches. The phonon relaxation times in the resistive scattering processes are shown in Fig. 3d.

### 3.3. Tin selenide (SnSe)

SnSe is a newly discovered thermoelectric material with a very high figure of merit (claimed to be as high as 2.6 at 923 K along the *b* axis) [26]. Its crystal structure is highly anisotropic and its good thermoelectric performance is mainly due to its intrinsically very low lattice thermal conductivity along *b* and *c* axes. At about 750 K, SnSe goes through a phase transition from the low-temperature *Pnma* structure to the high-temperature *Cmcm* structure. The high figure of merit values appear near and above the transition temperature. Here we calculate the lattice thermal

conductivity of the low-temperature phase and compared the results with the experimental measurements.

The phonon spectrum and lattice thermal conductivity of SnSe are shown in Fig. 4a and 4b, respectively. The calculated  $\kappa_L$  of SnSe using our method is more than twice the experimentally measured values in the temperature range of 300 K to 1000 K. The results of ShengBTE are also higher than experimental values, but are closer to them. Note, however, that experimental thermal conductivity values from Zhao et al. [26] are most likely significantly underestimated [27]. Nevertheless, it is clear, and our calculations confirm, that SnSe single crystal has a very low lattice thermal conductivity (around  $1 \text{ W m}^{-1} \text{ K}^{-1}$ ), the reason being a low phonon velocity and high Grüneisen parameter, especially for the *TA* branch (as shown in Table 1). In addition, extremely low characteristic temperatures of the acoustic and optical branches (Table 1) make its specific heat converge quickly to the classical Dulong–Petit constant value, and since the structure is relatively complex, there are many more optical phonons than acoustic phonons (Fig. 4c), but the former have much shorter relaxation time. This suggests a way to identify materials with likely low lattice thermal conductivity by looking for compounds with very low acoustic Debye temperature and complex structures with many atoms in the primitive cell.

In general, the method proposed in this work can give reliable results, especially for materials with normal and high lattice thermal conductivity (tens of  $\text{W m}^{-1} \text{ K}^{-1}$  and above) at temperatures  $>200 \text{ K}$ . Our approach does not require any experimental information and enables relatively cheap and accurate calculations.

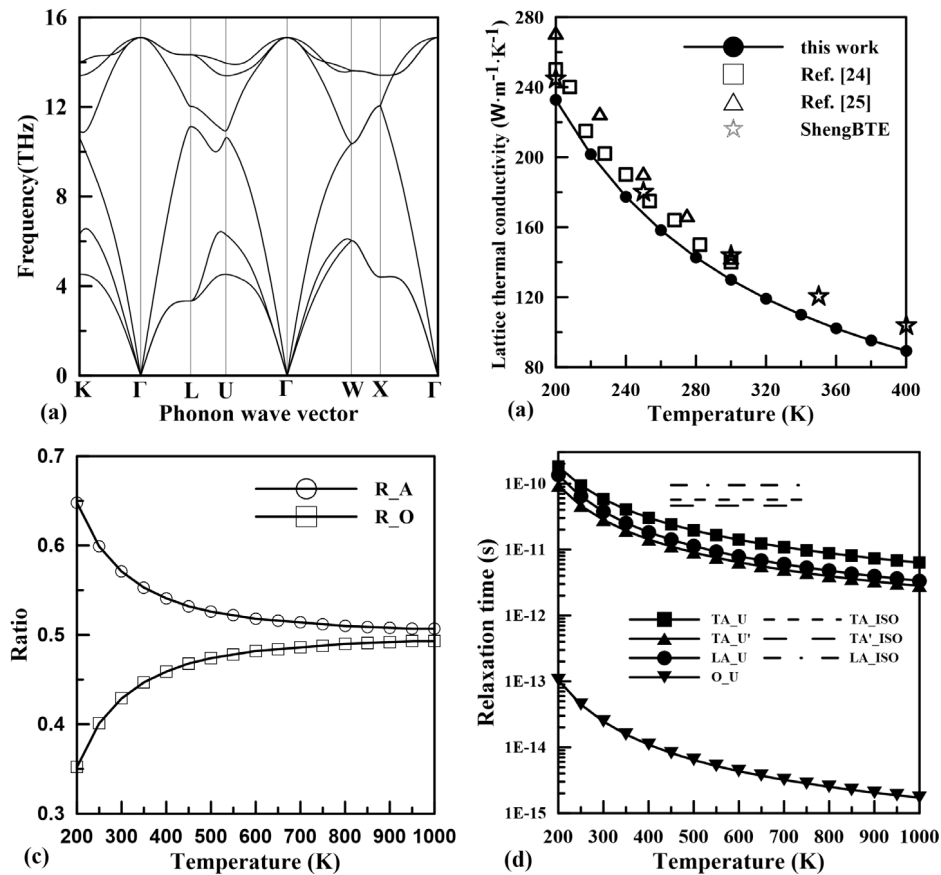


Fig. 3. (a) Phonon spectrum of Si. (b) Lattice thermal conductivity of Si calculated by our method, and compared with two experimental results. (c) Percentage of specific heat from the acoustic and optical branches in total specific heat of Si. (d) Phonon relaxation times for resistive scattering processes.

#### 4. Conclusion

We have presented a computer program AICON for calculating the lattice thermal conductivity using the modified Callaway–Callaway model. Going beyond the original Callaway model, we take into consideration the optical branches, using the specific heat ratio as a weight to sum the contribution of the acoustic and optical branches. Our method takes into account the phonon–phonon normal scattering, Umklapp scattering, and isotope scattering processes, while all the necessary parameters can be calculated using first-principles methods. The capability of our program has been demonstrated on three examples of isotropic and anisotropic systems, which included compounds with very high and very low thermal conductivity. All the reviewed cases validate the robustness and accuracy of our method.

Compared to fully *ab initio* program like ShengBTE, our program works much faster with the total calculation time three (or two) times that of a phonon spectrum calculation, since we do not need to calculate the computationally expensive anharmonic force constants. Our approach can be used for a wide range of materials and gives more accurate results compared with other semi-empirical methods. For different scattering processes, AICON directly estimates phonon relaxation times, providing additional information for studying the origins of thermal resistivity.

One of the shortcomings of the presented approach is that the optical branch is treated as a longitudinal acoustic branch, which is clearly a rough approximation. In reality, the optical branch has its own dependence on the frequency and temperature, which needs further theoretical investigation to find the proper formalism. The other issue comes from the original Debye–Callaway

model, where Callaway used the classical Boltzmann distribution to describe the phonon behavior. However, the Bose–Einstein distribution should be used for phonons, and the resulting equations may differ from the original ones. This has been addressed by Allen [28] and the modified formulas will be included in the future version of the presented method. We strongly encourage those who have similar research interests to join us and further develop this program.

Overall, our program will be useful for a high-throughput screening of the lattice thermal conductivity of materials.

#### Declaration of competing interest

The authors declare that they have no known competing financial interests or personal relationships that could have appeared to influence the work reported in this paper.

#### CRedit authorship contribution statement

**Tao Fan:** Conceptualization, Methodology, Software, Writing - original draft. **Artem R. Oganov:** Funding acquisition, Supervision.

#### Acknowledgments

The authors acknowledge the usage of Skoltech HPC cluster PARDUS for obtaining the results presented in this paper. This work is funded by Russian Foundation for Basic Research (grant 18-29-12128/18).

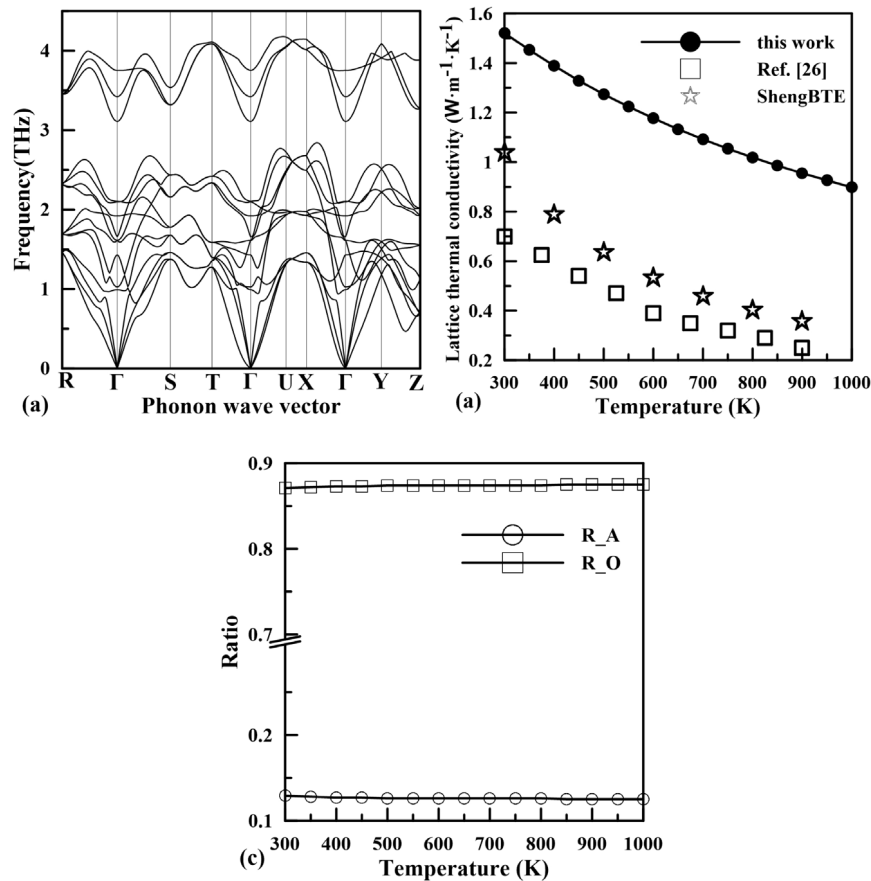


**Fig. 4.** (a) Phonon spectrum of SnSe. (b) Lattice thermal conductivity of SnSe calculated by our method in comparison with the experimental results. (c) Percentage of specific heat from the acoustic and optical branches in total specific heat of SnSe.

## References

- [1] A. Togo, L. Chaput, I. Tanaka, *Phys. Rev. B* 91 (9) (2015) 094306.
- [2] W. Li, J. Carrete, N.A. Katcho, N. Mingo, *Comput. Phys. Comm.* 185 (6) (2014) 1747–1758.
- [3] P.K. Schelling, S.R. Phillpot, P. Keblinski, *Phys. Rev. B* 65 (14) (2002) 144306.
- [4] A.J. McGaughey, M. Kaviany, *Adv. Heat Transfer* 39 (2006) 169–255.
- [5] D. McQuarrie, *Statistical mechanics* University Science Books, Sausalito, CA, 2000, pp. 222–223.
- [6] D.A. Broido, M. Malorny, G. Birner, N. Mingo, D. Stewart, *Appl. Phys. Lett.* 91 (23) (2007) 231922.
- [7] J. Callaway, *Phys. Rev.* 113 (4) (1959) 1046.
- [8] M. Asen-Palmer, K. Bartkowski, E. Gmelin, M. Cardona, A. Zhernov, A. Inyushkin, A. Taldenkov, V. Ozhogin, K.M. Itoh, E. Haller, *Phys. Rev. B* 56 (15) (1997) 9431.
- [9] D. Morelli, J. Heremans, G. Slack, *Phys. Rev. B* 66 (19) (2002) 195304.
- [10] Y. Zhang, *J. Materiomics* 2 (3) (2016) 237–247.
- [11] G.A. Slack, *Solid State Physics*, Vol. 34, Elsevier, 1979, pp. 1–71.
- [12] A. Togo, F. Oba, I. Tanaka, *Phys. Rev. B* 78 (13) (2008) 134106.
- [13] G. Kresse, J. Furthmüller, *Phys. Rev. B* 54 (11) (1996) 169.
- [14] P. Klemens, *Proc. Phys. Soc. A* 68 (12) (1955) 1113.
- [15] G. Kresse, J. Furthmüller, *Phys. Rev. B* 54 (16) (1996) 11169.
- [16] G. Kresse, J. Furthmüller, *Comput. Mater. Sci.* 6 (1) (1996) 15–50.
- [17] J.P. Perdew, K. Burke, M. Ernzerhof, *Phys. Rev. Lett.* 77 (18) (1996) 3865.
- [18] H.J. Monkhorst, J.D. Pack, *Phys. Rev. B* 13 (12) (1976) 5188.
- [19] X. Gonze, C. Lee, *Phys. Rev. B* 55 (16) (1997) 10355.
- [20] D. Onn, A. Witek, Y. Qiu, T. Anthony, W. Banholzer, *Phys. Rev. Lett.* 68 (18) (1992) 2806.
- [21] L. Wei, P. Kuo, R. Thomas, T. Anthony, W. Banholzer, *Phys. Rev. Lett.* 70 (24) (1993) 3764.
- [22] A. Ward, D. Broido, D.A. Stewart, G. Deinzer, *Phys. Rev. B* 80 (12) (2009) 125203.
- [23] J. Carrete, B. Vermeersch, A. Katre, A. van Roekeghem, T. Wang, G.K. Madsen, N. Mingo, *Comput. Phys. Comm.* 220 (2017) 351–362.
- [24] R. Kremer, K. Graf, M. Cardona, G. Devyatikh, A. Gusev, A. Gibin, A. Inyushkin, A. Taldenkov, H.-J. Pohl, *Solid State Commun.* 131 (8) (2004) 499–503.
- [25] Y.S. Touloukian, R. Powell, C. Ho, P. Klemens, *Thermophysical Properties of Matter—the Tprc Data Series. Volume 1. Thermal Conductivity—metallic Elements and Alloys*, Tech. rep., THERMOPHYSICAL AND ELECTRONIC PROPERTIES INFORMATION ANALYSIS CENTER LAFAYETTE IN, 1970.
- [26] L.-D. Zhao, S.-H. Lo, Y. Zhang, H. Sun, G. Tan, C. Uher, C. Wolverton, V.P. Dravid, M.G. Kanatzidis, *Nature* 508 (7496) (2014) 373.
- [27] P.-C. Wei, S. Bhattacharya, J. He, S. Neeleshwar, R. Podila, Y. Chen, A. Rao, *Nature* 539 (7627) (2016) E1.
- [28] P.B. Allen, *Phys. Rev. B* 88 (14) (2013) 144302.